DEGRADATION OF HIGH VOLTAGE SOLAR ARRAY DUE TO ARCING IN LEO PLASMA ENVIRONMENT

Teppei Okumura
Department of Electrical Engineering
Kyusyu Institute of Technology
1-1 Sensui Tobata-ku Kitakyusyu 804-8550,Japan
Phone: +81-93-884-3228
Fax: +81-93-884-3228

Satoshi Hosoda
Kazuhiro Toyoda
Mengu Cho
Department of Electrical Engineering
Kyusyu Institute of Technology, Japan

Abstract

A degradation test for a solar array coupon against ESD was performed under simulated Low Earth Orbit environment. All tests were performed in a vacuum chamber with a plasma source. A test coupon was biased at -400V with the aim of developing the next generation 400V high voltage solar array. The LCR circuit was used in order to simulate the arc current that flows by gathering the charge stored on coverglasses. Tests were repeated until the solar array coupon was damaged. The arc locations and waveforms of both current and voltage were detected for all the arcs during the tests. The electrical performance of the coupon was measured after every test without opening the vacuum chamber. Many arcs occurred and caused the cell degradation. The cell was damaged by only one arc that occurred at the edge of cell, not at electrodes.

Introduction

The spacecrafts, such as satellites and space station, have larger structures and longer lifetimes year after year. These spacecrafts need a large amount of the electric power generation, nowadays up to several kW power level. The International Space Station (ISS) can generate 65kW electric power. The higher bus voltage is indispensable for the large spacecrafts to reduce both the increase in power line's weight and the power loss resulting the joule heating due to the increase in electric power generation. The bus voltage over 100 V is employed for the kW class spacecrafts, and the output voltage of the solar array becomes over 100 V. In the case of ISS, the electric power is generated at the voltage of 160 V by the solar array, and is transmitted at 120 V. In near future, the electric power will increase when the lager spacecrafts appear. Taking into account that the bus voltage is generally proportional to the square root of the electric power, the spacecrafts generating the 1 MW class electric power need the output voltage of about 400 V.

The negative end of the solar array is connected to the spacecraft body in many spacecrafts. Under the Low Earth Orbit (LEO) environment, the space plasma, whose density is on the order of 10^{10}~10^{12} m^{-3}, can charge the spacecrafts at the negative potential with respect to the plasma, because of electron's higher velocity than ions. When the positive end of the solar array has the same potential as the ambient plasma, the spacecraft body and the negative end of the solar array have the negative potential equal to the voltage in power generation.

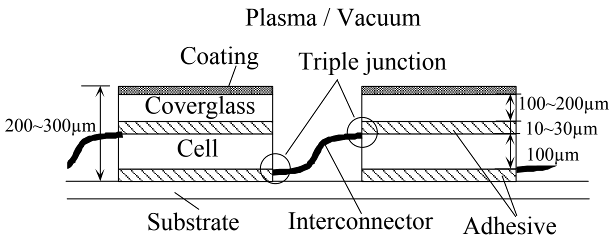

Figure 1. Cross-section of the solar array.

When the solar array generates the electric power at 400 V, almost part of the spacecraft and the solar array have negative potential with respect to the plasma, and especially the negative end of the solar array is –400 V.

The arcing is observed on the spacecraft and the solar array, when the spacecraft has the negative potential of from 100 V to 200 V with respect to the ambient plasma [1]. The arcing can cause the degradation of the solar cells, the malfunction of the electrical devices, and the short-circuit of the solar array circuit [2]. The influences on the solar array due to the arcing depend on both the number and the energy of arcs. The more negative the spacecraft is charged, the higher the arc rate becomes because the potential difference between the coverglass and the conductor increases. The arc energy also becomes larger so that the energy depends on the amount of the positive charge gathered from the charged coverglass (dielectric) during arcing.

The cross-sectional view of the solar array for space use is shown in Fig. 1. The solar cells are glued on the Kapton substrate by adhesive, and connected in series each other by the interconnectors (conductor). The coverglasses are also glued on the cells. When the spacecraft has negative potential with respect to the plasma, the cells and the interconnectors also have negative potential. Therefore ions are attracted to cells and attack the coverglasses. The coverglass surface is charged to positive by ions. This potential difference between the coverglass and the interconnector enforces the electric field at the triple junction, which consists of the interconnector, the coverglass, and plasma. The electrons emitted by the field emission from the triple junction collide with the side wall of the coverglass. The electric field is enforced by the charging of the coverglass. As the result, an arc occurs.

So far, we had developed the 400V high voltage solar array on LEO environment [3,4]. From this result, it was verified that the most effective techniques of mitigating arcs was to cover the coupon with a transparent film. This coupon could suppress the arcing completely up to the negative potential of –1000 V. However in space, the space debris can attack the solar array and make a hole on the film. In such case, it is difficult to suppress completely arcing on the solar array. Therefore for both the mitigation of the solar array degradation and the power generation system design containing the solar array in the spacecraft, it is important to investigate whether the solar array is degraded or not by arcing, and what degree the solar array is degraded.

The purpose of this study is to investigate the degradation of the 400 V high voltage solar array in LEO.

Charge Supplied by the Charged Coverglass

Before arcing, the surface of the coverglass (a dielectric with 100µm thicness) has the positive potential with respect to the cell and the interconnector, because the coverglass surface has almost same potential as the plasma though most part of the spacecraft has the negative potential with respect to the plasma. After arcing, the charge stored in the capacitance between the spacecraft and the plasma is discharged, and the spacecraft potential rises up to the plasma potential. Then the coverglass surface becomes positive against the plasma. The arc plasma spreads from the arc site with neutralizing the charge on the coverglass. This neutralization of the coverglass charge is observed in the ground tests. The maximum size of the coupon used for such an experiment is 1m square because of the spatial limit of the experimental facility on the ground [5]. For real space use, in the case of ETS-VIII which generates 8 kW at 110V for example, one wing of the solar array is about 10 m in length [6]. The solar array operating at 1MW at 400V will have a large number of solar cells and a huge area. Many coverglasses exist (capacitance) on this large area of the solar array and can supply a lot of charge to the arc plasma in arcing. It is important for the degradation test to estimate the charge supplied from the coverglasses, since it is thought that the degree of the cell damage due to arcing depends on the amount of the charge flowing to the arc site. Then we estimated the amount of the charge neutralized by the arc plasma on the basis of the experimental result [7].

In this experiment, it was observed that the arc plasma could neutralize the charge stored on the film which simulated the coverglass and was placed at 4m far from the arc site. Therefore it was assumed that the arc plasma could neutralize the charge of the coverglass within 4m from the arc site [7]. It was also assumed that the ratio of the neutralized charge to the total charge stored on the coverglass, γ_c, was 100% at the arc site, and was inversely proportional to the distance from the arc site, r, and was 0% at 4 m from the arc site. The velocity of the arc propagating with neutralizing the charge on coverglass was 7×10^4 m/s from the experimental result. We also put the capacitance of the coverglass to C_{cg}=286.5 nF/m^2.

The charge on the coverglass is neutralized radially at the velocity, v, from the arc site. The charge, $C_{cg}|\Delta V|$, is stored on the coverglass per unit area before arcing, where ΔV is the potential difference between the coverglass and the cell. We put that $\gamma_c = 1 - 0.25r$ on the condition, γ_c=0 at r=4 m, where r represents m in unit. The time duration from the beginning of arcing is t s. We also put the charge neutralized at r during dt to dC, and from $r = vt$, the discharge current, I, is

$$I = \frac{dC}{dt} = \frac{(\pi(r+dr)^2 - \pi r^2)C_{cg}|\Delta V|\gamma_c}{dt} \tag{1}$$

$$\cong 2\pi r C_{cg}|\Delta V|\gamma_c \frac{dr}{dt} \tag{2}$$

$$= 2\pi C_{cg}|\Delta V| v^2 t(1 - 0.25vt) \tag{3}$$

Substituting the value of the constant, we have

$$I = 3.52 \times 10^6 t(1 - 1.75 \times 10^4 t), \text{ A} \tag{4}$$

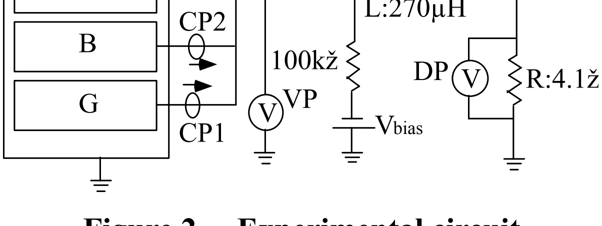

Figure 2. Experimental circuit.

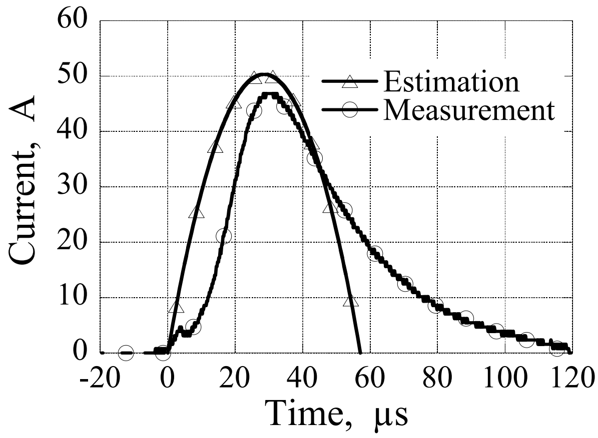

Figure 3. Waveform of arc current.

From this equation, the peak of the arc current, I_{max}, is 50 A, and the amount of the charge is 2 mC. In the previous experiment, the external capacitance was connected to the circuit to simulate the coverglass capacitance. In this method, the charge stored in the external capacitance flows via the arc plasma with several Ω between the solar array and the camber wall in the arc inception. Therefore the charge flows during such short time as a few microseconds, the peak of the current is very large. Then we controlled the discharge current close to Eq. (4) by means of adding a resistance and an inductance besides a capacitance to the circuit. The experimental circuit is shown in Fig. 2. The voltage of –400 V was applied to the solar array during the experiment. The capacitance of 5 µF was used so as to set the charge to 2 mC. The inductance, H, is 270 µH, and the resistance, R, is 4.1 Ω. These values were estimated by a circuit simulator in advance of the experiment and were corrected slightly by the experiment. The circuit showed the waveform of the discharge current (Fig. 3).

The peak of the discharge current was 47 A in Fig. 3 and was close to the estimated value, 50 A. This circuit could suppress the large current such as the rush current over 100 A. The amount of charge was about 2 mC, and all amount of the charge stored in the capacitance was discharged during arcing.

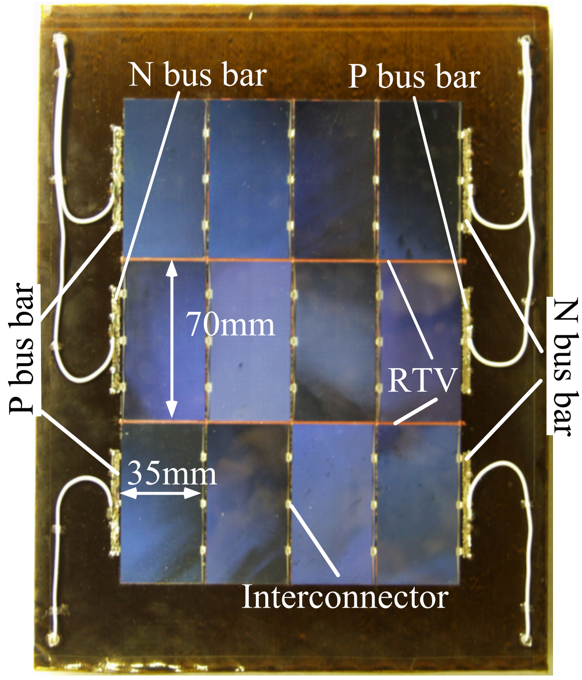

Figure 4. Picture of the coupon.

Experiment

Solar array coupon

The picture of the solar array coupon used in the experiments is shown in Fig. 4. This coupon is the basic design for the 100 V solar array used currently in the space. The substrate is 25 mm aluminum honeycomb which is covered with Carbon Fiber Reinforced Plastics (CFRP), and the top of the substrate is covered with the Kapton film. The twelve silicone cells (70mm$\times$35mm) are glued on the Kapton film. Four cells are connected in series by the interconnectors. The electrodes of both end of the series connection are called the bus bars. Three parallel connections are called as R, B, G strings, respectively. We also call the cells by the numbers as shown in Fig. 4. The cells have IBF (Integration Bypass Fumction), which allows the current flow from N to P electrode in the cell even if the cell can not generate the electric power. The gap between strings are glued by RTV (Room Temperature Vulcanizing) silicone rubber to prevent the sustained arc [8, 9].

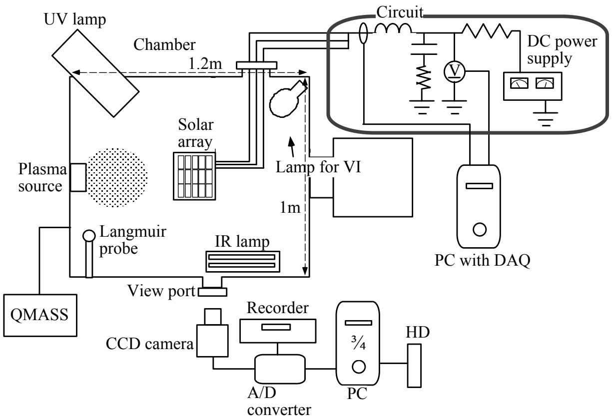

Figure 5. Experimental setup.

Measurement system

The sketch of the measurement system is shown in Fig. 5. The experiments were performed in a vacuum chamber, which was 1 m in diameter and 1.2 m in length. The pressure in the chamber could reach up to about 5×10^{-4} Pa, and was 1×10^{-2} Pa during the experiments. The plasma was produced by an ECR plasma source [10]. The plasma density around the coupon was about 5×10^{12} m^{-3} and the electron temperature was about from 3 eV to 7 eV with xenon gas of 2×10^{-8} kg/s. The coupon was kept at 40 ºC by an IR lamp to simulate the temperature on orbit during the experiment.

The arc location on the coupon was identified by a position identification system of arc discharge [11]. During the experiments, the video image of the coupon was recorded in a hard disk drive connected to a PC as the digital video image. After the experiments, the arc location was identified by means of analyzing the digital video image with a computer program in the PC.

All waveforms of the array potential and the discharge current were acquired by a high speed data acquisition system [12]. This system consists of a high speed data acquisition board, a PC, and a LabVIEW program, and can record the waveforms within about 30 ms intervals after a waveform is recorded. This system can also perform the real-time recording and display of the peak, the amount of charge, and the pulse width of the discharge current.

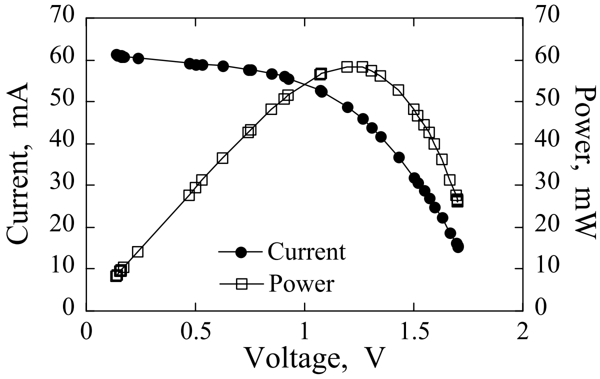

Figure 6. VI Characteristic.

The circuit used in the experiments is shown in Fig. 2. Here the current probes, CP1 and CP2, were HIOKI 3274 (DC ~ 10 MHz). The current supplied from the capacitance C was measured by measuring the potential of R using the differential probe DP.

The metal halide lamp mounted in the chamber enabled to acquire the electrical performance of the coupon without opening the chamber during the experiments. The electrical performance was acquired in each string by means of measuring both the output voltage and current with shifting the value of resistance connected to the string (VI characteristics). The example of the VI characteristic is shown in Fig. 6. The output power is also shown in this figure. The maximum power gives the electric performance of the strings. The illumination of this lamp was 19000 lx at the center of the coupon. The plasma source was stopped during the VI measurement. The VI curve was corrected by the coupon temperature, which was measured simultaneously, since the electric performance of the solar cell depended on its temperature.

Table 1 Test conditions.

Work gas	Xe
Mass flow rate	0.2 sccm
Plasma density	5×10^{12} m^{-3}
Chamber pressure	9.7×10^{-3} Pa
Neutral density	2.3×10^{18} m^{-3}
Bias voltage	-400 V
Array temperature	40 ºC
External capacitance	5 μF

Result and discussions

The experimental condition is listed

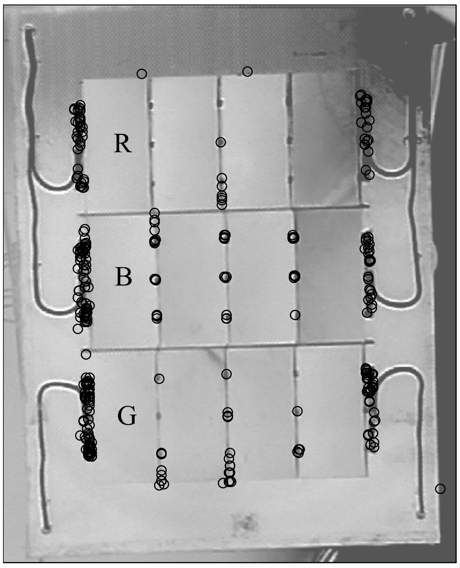

Figure 7. Position of arc.

Table 2. Experimental result.

Case	Experimental duration, s	Number of arcs		
		Total	Electrode	Cell edge
1	100	53	53	0
2	62	29	29	0
3	26	18	18	0
4	40	28	26	2
5	39	25	23	2
6	78	41	38	3
7	37	18	18	0
8	76	34	30	4
9	55	26	19	7
10	52	23	15	8
Total	565	295	269	26

in Table 1. The work gas of the plasma source was xenon, and the plasma density at the center of the coupon was about 5×10^{12} m^{-3}. Table 2 shows the experimental result, and Fig. 7 shows the arc location on the coupon during the experiments. The coupon was biased at –400 V in the plasma environment. The experimental case contains about 20 arcs, and was repeated until the coupon was degraded. After each experimental case, the electric performance was acquired by the VI measurement without opening the chamber. The 10 cases were performed totally, and the total experimental time was 565 s, the total number of arcs was 295. The 269 arcs of all arcs occurred at the electrodes, like the bus bar and the interconnector, which were exposed to the space, and the 26 arcs occurred at the side edges of the cells except for the exposed electrode. This result showed that the arc occurred easier at the exposed electrode than at the cell edge.

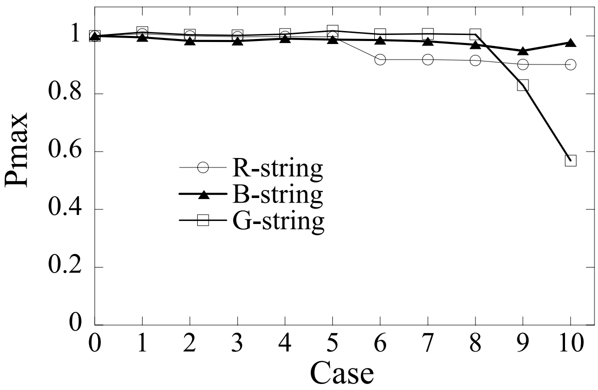

Figure 8. Peak of output power.

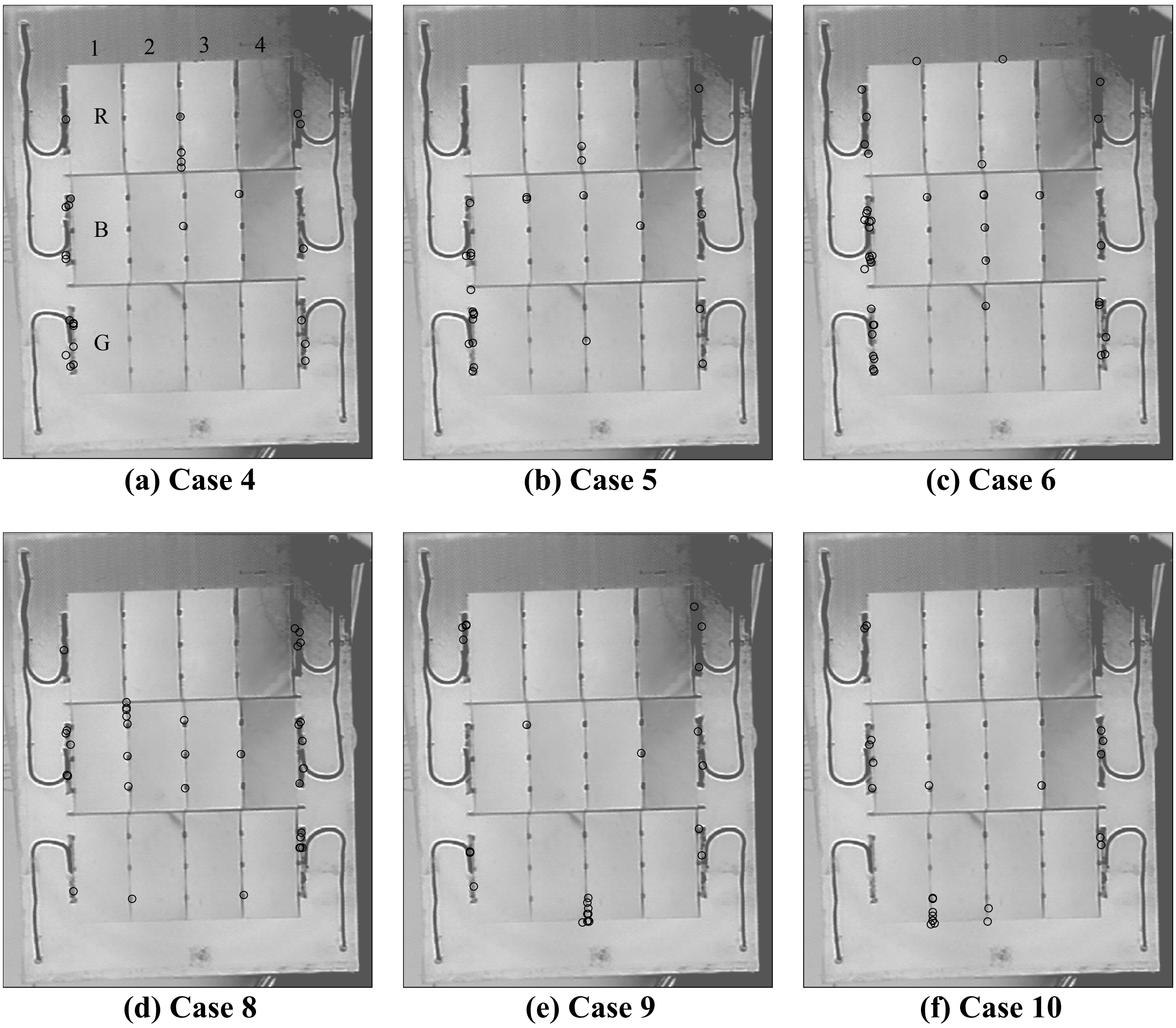

(a) Case 4 **(b) Case 5** **(c) Case 6**

(d) Case 8 **(e) Case 9** **(f) Case 10**

Figure 9. Position of arcs.

The peak of the output electric power measured after every case was shown in Fig. 8. The maximum power was normalized by the value measured before the experiment. The maximum power did not change in any strings by case 5. After case 6, the R-string showed degradation of electric power. After case 9, the G-string suffered the degradation of 20 %, and then suffered moreover the 20 % degradation after case 10. After all, the total power degradation was 40 % in the G-string.

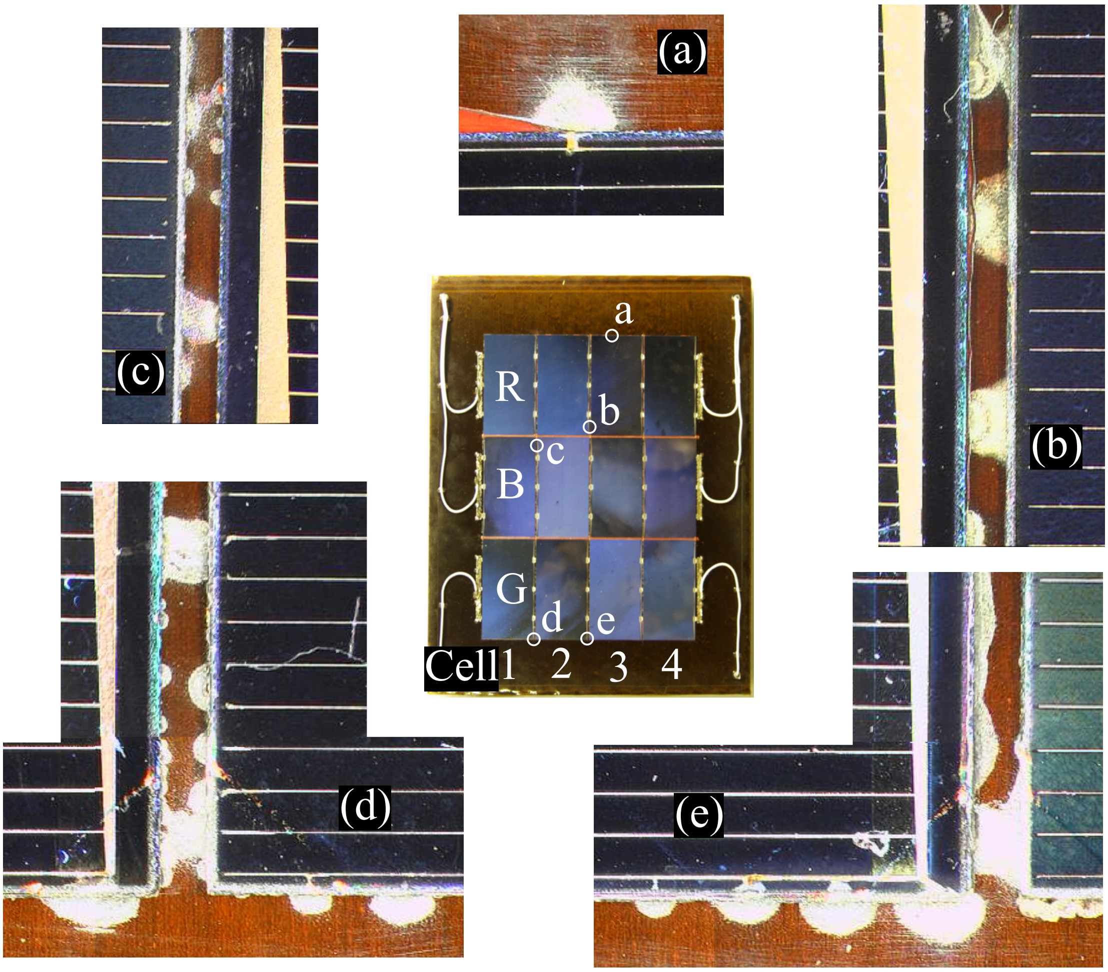

Figure 10. Microscopic picture at the cell edge.

The arcs occurred at the side edge of the cells in both R and G-strings, when the electric power of the strings was degraded. The distributions of the arc location in the cases 4, 5, 6, 8, 9, and 10, which had the arcs occurred at the side edge of the cells, are shown in Fig. 9. In the cases 4 and 5, three arcs occurred at the cell edge between the cells No. 2 and No. 3 in the R-string. In case 6, an arc occurred at the same position as cases 4 and 5, and at the top of the cell No. 1 and 3 in the R-string, respectively. No arc at the cell edge except for the cell edge between the cells occurred until case 6, and no degradation also occurred until case 6. In case 8, the cells were not degraded, though 4 arcs occurred at the cell edge between No. 1 and No. 2 in the B-string. In case 9, 7 arcs occurred in the G-string totally at the cell edge between No. 2 and No. 3, and at the bottom edge, and then the cells were degraded. In case 11, the arcs occurred in the G-string at the cell edge between No. 1 and No. 2, between No. 2 and No. 3, and at the bottom edge of both No. 1 and No. 2., and then the electric performance decreased moreover. It was verified that the arcs at the electrode exposed to the space did not degrade the cells, however the arcs at the side edge of the cells could degrade the cells.

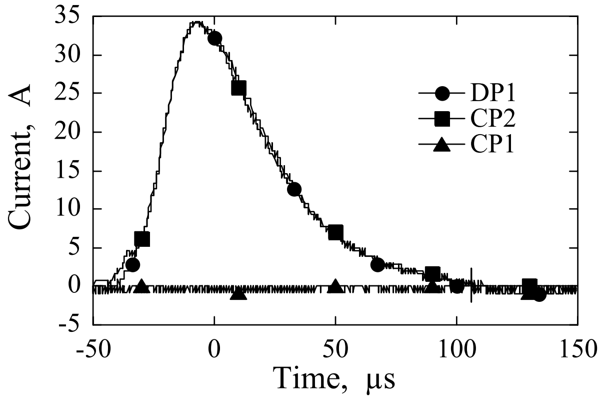

Figure 11. Waveform of the arc degrading the cell.

Figure 10 shows the microscopic picture of cells that had arcs at their side edge. Each position of the cell edge was named as (a) ~ (e). The P electrode was melted out of the backside of the cell in the case of arcing at the cell edge. When the arcs occurred at the exposed electrode like the interconnector, there was no such an arc track.

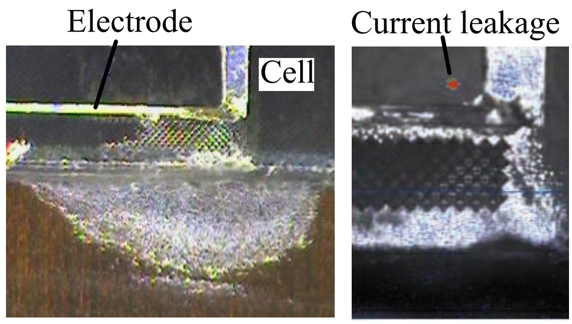

Figure 12. Microscopic picture of current leakage point.

At most of the positions where the arcs occurred at the cell edge between the cells, the cell seems to be connected to the adjacent cell by the arc site. If the P electrodes of the backside of the cells are short-circuited each other, the P and N electrodes are short-circuited in one cell, and this leads to the decrease in electric power. The arc sites between the cells were observed in all strings. To clarify whether two cells were short-circuited or not, the resistance was measured between the adjacent cells, No. 1 and No. 2 in the G-string. The three interconnectors connecting two cells were cut in order to measure the resistance. The result showed that the insulation was kept between the two cells. From this result, the decrease in electric power resulted from the short-circuit of the PN junction in the cell.

In case 6 which the R-string was degraded in, the arcs occurred at the top edge of the cells besides at the gaps between cells. As shown in Fig. 10 (a), an arc site attached at the top edge by the arcing at the cell edge. The parallel lines in this picture were the N bar electrodes at the cell surface, and were insulated from the space by the coverglass. In Fig. 10 (a), the N electrode seemed to be connected to the cell edge by the arc site. In the R-string, such an arc site from the N electrode between the coverglass and the silicon was observed only in Fig. 10 (a). In the B-string, there was no arc site like this.

In the G-string, both the power degradation and the arcing at the cell edge occurred in cases 9 and 10. The arc sites like Fig. 10 (a) were also observed in the G-string, one arc site in the cell No. 1, and five arc sites in No. 2. The position of the current leakage in the cell was identified.

At first, in the G-string, the degraded cells were identified by measuring the open-circuit voltage (Voc) of each cell with exposing one cell to the light and shading the other cells. The Voc of the cells No. 1 and 2 was about the one tenth of the other cells, and these cells were identified as the degraded cells. This result was consistent with the arcs occurring at the cell edge of these cells.

Table 3. Parameters of arcs.

Variable	Minimum	Maximum	Points	Mean	Std Deviation
I_{max}, A	13.7	46.1	289	37.5	7.42
Charge, mC	0.98	2.00	289	1.73	0.23
Pulse width, μs	97	154	289	111	8
V_0, V	-389	-201	289	-347	46

Next, the current leakage position was identified in the No. 1 cell identified as the degraded cell. The identification method was identified by detecting the IR radiation from the leaking position with applying the inverse voltage to the string. The identified current leakage position is shown in Fig. 11. This position corresponds to the bottom edge in Fig. 10 (d). The current leakage position identified in the No. 1 cell was only one place shown in Fig. 11. From the arc location identification result, the only one arc occurred at the arc site in Fig. 11, and this arc caused the power degradation of the No. 1 cell. From this result, it was confirmed that only one arc could destroy the PN junction in the cell.

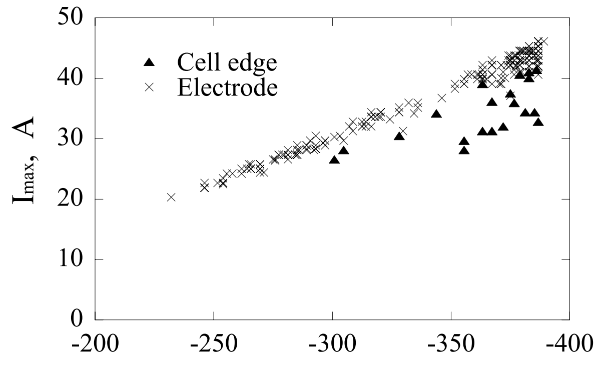

Figure 13. Relation between I_{max} and V_0.

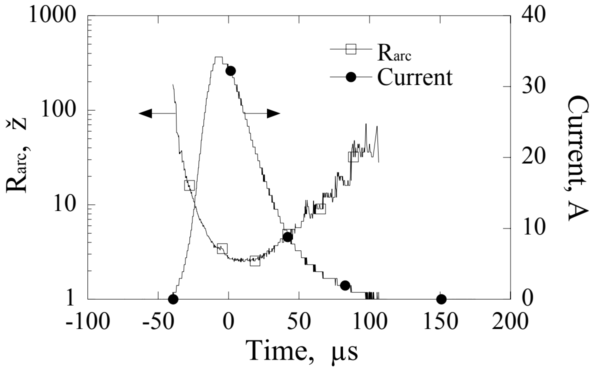

Figure 14. Waveform of R_{arc} and current.

The current waveforms of the arc, which occurred at the bottom edge of the No. 1 cell and caused the current leakage in the cell, was shown in Fig. 12. These current waveforms in this figure were measured by the differential probe DP and the current probes CP1 and CP2 in the circuit (Fig. 2). Table 3 lists the quantities, the minimum, the maximum, the average, and the standard deviation for the peak value of the current, the amount of the charge, the pulse width, and the array potential before arcing, respectively. Here the charge and the pulse width were calculated for the waveform within 95 % of the peak value of the current. The discharge current flew in G-string where the emission of the arc was observed. The current waveform of this arc which destroyed the cell was similar to other arcs, and the peak value of the current was 34 A, the amount of the charge was 1.2 mC, the pulse width was 116 μs, and the array potential before arcing was –381 V.

As shown in Table 3, the current waveform in Fig. 12 was the average value with no difference from the other arcs. Since it takes finite time to charge the capacitance from 0 V to –400 V after arcing when the arc rate becomes high, the arc can occur before the array potential reaches to –400 V. Therefore the array potential before arcing, V_0, has various values. Figure 13 shows the relation between the V_0 and the I_{max} for the arcs at the cell edge and at the interconnector or the bus bar, respectively. Naturally, the V_0 was proportional to the charge stored in the external capacitance before arcing, Q_0. If the Q_0 is large, the I_{max} becomes large, too. In the case of the arcs at the electrodes, the $|V_0|$ was proportional to the I_{max}. On the contrary, the I_{max} of the arcs at the cell edge was smaller than the arcs at the electrodes. This means that the resistance R_{arc} between the array (cathode) and the vacuum (anode) was larger in arcs at the cell edges than in arcs at the electrodes.

To investigate R_{arc} in detail, the waveform of R_{arc} was calculated by means of dividing the absolute value of array potential by the current. The example waveform of R_{rac} is shown in Fig. 14. The R_{arc} decreased after arcing and was minimum after the current was maximum, and then increased. This resistance is the sum of the resistance between the array and the chamber via plasma, and the resistance in the array circuit including the inside of cells. The minimum value of R_{arc} was put as R_{arc_min} and was calculated over all discharge waveforms.

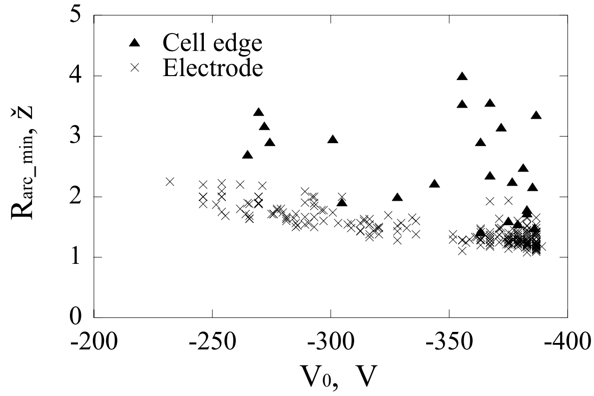

Figure 15. Relation between R_{arc_min} and V_0.

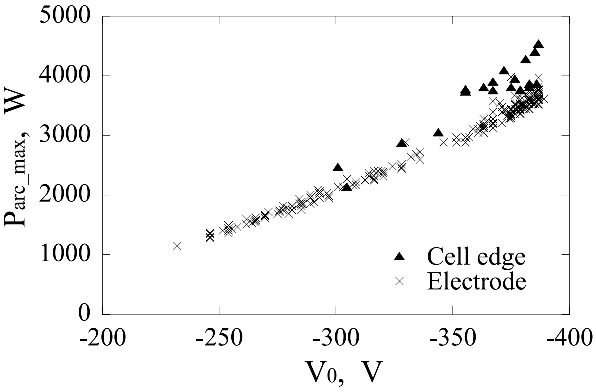

Figure 16. Relation between Parc_min and V0.

Figure 15 shows the relation between R_{arc_min} and V_0 for the arc both at the cell edge and at the electrode. In the case of the arcs at the electrode, R_{arc_min} showed a tendency to decrease with increase in $|V_0|$. The resistance between the electrode and the chamber decreases with increase in the energy of electrons emitted from the electrode. Therefore the resistance decreased since the energy of electrons accelerated from the cathode was large with increase in $|V_0|$. The resistance was larger in the cell edge arcs than in the arcs at the electrode. In the case of the arc that degraded the cell (Fig. 11), the V_0 was –384 V, and the R_{arc_min} was 2.5Ω. The average of R_{arc_min} at the electrode over 350 V of $|V_0|$ was 1.3Ω, and the R_{arc_min} in the case of the arc degrading the cell was about 1Ω larger than in the cell edge case. It is one of this reason that the electrons were emitted easier from the electrode exposed to space than from the P electrode at the backside of the cell between the cell and the substrate. The P electrode was melted out from the backside of the cells in the case of the cell edge arcs, though the interconnectors were not damaged by the arcs. From these results, the cell can be heated from the arc as the arc occurred at the cell edge.

To investigate the heat energy supplied to the cell by arcs, the power P_{arc} wasted by R_{arc} was calculated by multiplying the current and the array potential. In Fig. 16, the maximum P_{arc}, P_{arc_max} , was plotted against V_0. As shown in Fig. 16, the P_{arc_max} of the cell edge arcs was larger than that of the electrode arcs. This result means that the cell edge arcs can heat the cell harder than the electrode arcs. It is thought as one of the reasons for the cell degradation that the cell edge arcs heated the cell locally and melted the cell edge and then short-circuit PN junction of the cell.

In the experiment, the arc site between the coverglass and the silicone cell was observed at the current leakage point. If the adhesive between the coverglass and the cells is absence, the arc current can flow into N electrode as an arc occurs at the cell edge. The N+ diffusion layer just under the adhesive is about 0.1 μm in depth. Since this layer can be destroy easily by the arc site, PN junction is short-circuited. This is one of the reasons for the cell degradation.

The array was biased at –400 V in the experiment, and the arcs caused the power degradation. The power degradation was 10 % in the R-string, and 40 % in the G-string. Because of 4 cells in each string, the 2 cells were destroyed totally. The 295 arcs occurred during the experimental time of 565 s. From this result, the probability of one arc destroying one cell is about 0.7 %. Limiting at the cell edge, 26 arcs occurred. The probability of one cell edge arc destroying one cell is high, about 7.7 %. Since the arc rate decreases with time, and the plasma density in the experiment is the maximum value in LEO, to estimate the degraded cells in the satellite lifetime is overestimation. We can estimate that 5.7×10^5 cells are degraded during the lifetime of 10 years using the probability of 0.7 %. Generating the power of 1 MW at 400 V, the number of the silicon cell generating 1 A at 0.5 V is 2×10^6, the series of 800 cells and 2500 string. A fourth of all cells is destroyed. This degradation is harder than the radiation degradation. In real case of 400 V power generation, the arc mitigation methods must be applied to the coupon. However, it is difficult for these methods to mitigate arcs completely. From these results, the double mitigation method, which means that the arc do not occur at the cell edge if the arc occur, is needed.

Conclusions

The ESD test of the 400 V power generation solar array for space use was performed in the vacuum chamber simulating the LEO plasma environment. The waveform of arc current was controlled close to the waveform considering the neutralization by arc plasma of coverglass charge by means of using LCR circuit. The system, which can measure the electrical performance of the solar array without opening the chamber, was constructed.

A lot of arcs occurred on the solar array biased at –400 V and caused the degradation of the electric performance of solar array. From the results of identifying the degraded cells and current leakage point of the cells, it was observed that only one arc destroyed the PN junction of the cell. The arc destroying the cell occurred at the cell edge but at the electrode exposed to space. The interconnector and the bus bar had little damage due to arcing. On the other hand, as the arcs occurred at the cell edge, the P electrode melting out from the backside of cell, and the arc site between coverglass and the silicone were observed. From these results, it was thought that the arcs at the cell edge added heat stress locally to the cell edge and could destroy the cell.

In real use of the high voltage solar array in space, it is necessary to apply the mitigation method to the solar array. In addition of applying the mitigation method, it is is important to prevent the arcs at the cell edge if the arc occurs on the solar array.

Acknowledgement

This study is carried out as a part of Grants-in-Aid for Scientific Research by JSPS and "Ground-based Research Announcement for Space Utilization" promoted by Japan Space Forum.

References

1. Grier, N. T.: Plasma Interaction Experiment II (PIX II): Laboratory and Flight Results, Spacecraft Environmental Interaction Technology-1983, NASA CP-2359, 1985, pp.333-347.

2. Katz, I., Davis, V. A. and Snyder, D. B.: Mechanism for Spacecraft Charging Initiated Destruction of Solar Arrays in GEO, AIAA paper 98-1002, 36th Aerospace Sciences Meeting, Reno, 1998.

3. Cho, M., Shiraishi, K., Toyoda, K., Hikita, M.: Basic Developmental Experiment of Arc-Resistive High Voltage Solar Array for Low Earth Orbit, Journal of the Japan Society for Aeronautical and Space Sciences, Vol.50, No.581, (2002), pp.215-222.

4. Toyoda, K., Saionji, A., Cho, M., and Hikita, M.: Experimental Study of Mitigating Arcs on a High Voltage Solar Array in LEO, Proceedings of the 23rd International Symposium on Space Technology and Science, Matsue, Japan, 2002, pp. 379-384.

5. Leung, P.: Plasma Phenomena Associated with Solar Array Discharges and Their Role in Scaling Coupon Test Results to a Full Panel AIAA 2002- 0628, 40th Aerospace Sciences Meeting, Reno, January, 2002

6. Meguro, A., Tsujihata, A., Hamamoto, N., and Homma, M.: Technology status of the 13 m aperture deployment 21 antenna reflectors for Engineering Test Satellite VIII, Acta Astronautica, Vol. 47, No. 2 (2000), pp. 147-152.

7. Cho, M., Miyata, N., Hikita, M., and Sasaki, S.,: Discharge over Spacecraft Insulator Surface in Low Earth Orbit Plasma Environment, IEEE Transactions on Dielectrics and Electrical Insulation, Vol.6, No.4 (1999), pp. 501-506.

8. Cho, M., Ramasamy, R., Matsumoto, T., Toyoda, K., Nozaki, Y., Takahashi, M.,: Laboratory Tests on 110-Volt Solar Arrays in Simulated Geosynchronous Orbit Environment, Journal of Spacecraft and Rockets, Vol. 40, No. 2 (2003), pp. 211-220.

9. Cho, M., Ramasamy, R., Toyoda, K., Nozaki, Y., Takahashi, M.,: Laboratory Tests on 110-Volt Solar Arrays in Ion Thruster Plasma Environment, Journal of Spacecraft and Rockets, Vol. 40, No. 2 (2003), pp. 221-229.

10. Hayashi, H., Saionji, A.,Toyoda, K., Cho, M., and Kuninaka, H.: Development of Plasma Interaction Acceleration Test Facility for Study on Space Material Deterioration, 23rd Int. Symp. Space Tech. Sci. ISTS 2002-b-28, Matsue, Japan, 2002.

11. Toyoda, K., Cho, M., and Hikita, M.: Development of Position Identification System of Arc Discharge on a Solar Array in Vacuum by Digital Processing of Video Images, Journal of the Japan Society for Aeronautical and Space Sciences, Vol.51, No.589, (2003), pp. 82-84.

12. Saionji, A., Toyoda, K., and Cho, M.: Development of Automatic Data Recording and Analysis System for Laboratory Experiments on High Voltage Solar Array in Space Environment, Proceedings of ACED & K-J Symp. on ED and HVE, Seoul, 2002, pp.63-66.